Roles of human SPATA3 in cell proliferation and expression pattern of *Spata3* in mouse testis

LI FU[1-3*], BAIXU ZHOU[1,4*], XIA JIANG[1-3], JINGLIANG CHENG[1], QIANG WU[3] and JUNJIANG FU[1]

[1]Key Laboratory of Epigenetics and Oncology, The Research Center for Preclinical Medicine, Southwest Medical University, Luzhou, Sichuan 646000, P.R. China; [2]Department of Reproductive Medicine, The Affiliated Hospital, Southwest Medical University, Luzhou, Sichuan 646000, P.R. China; [3]The State Key Laboratory of Quality Research in Chinese Medicine and Faculty of Chinese Medicine, Macau University of Science and Technology, Macau SAR 999078, P.R. China; [4]Department of Gynecology and Obstetrics, Guangzhou Women and Children's Hospital, Guangzhou, Guangdong 510623, P.R. China

Received January 15, 2025; Accepted June 10, 2025

DOI: 10.3892/mmr.2025.13620

Abstract. Male infertility predominantly manifests as abnormal spermatogenesis and maturation, abnormal semen quality, chromosomal abnormalities, and endocrine dysfunction. The present study aimed to explore the role, expression pattern and localization of spermatogenesis-associated protein 3 (SPATA3) in the testis, and to analyze its spatiotemporal expression and function. Using previously acquired plasmids as templates, recombinant plasmids of different SPATA3 isoforms were constructed. Cell Counting Kit-8 assay was used to analyze cell proliferation. Reverse transcription-PCR and western blotting were used to determine the mRNA and protein expression levels, respectively. Different SPATA3 isoforms were induced to be overexpressed, among which SPATA3-I1 and SPATA3-I2 promoted cell proliferation. The subcellular localization results indicated that the green fluorescent protein fusion proteins of various isoforms were mainly localized in the nucleus. However, the fluorescence of the fusion proteins pEGFP-C3-SPATA3-I3 and pEGFP-C3-SPATA3-I4 tended to be distributed in the cytoplasm, accompanied by a decrease in nuclear fluorescence. Additionally, the SPATA3-I2 isoform protein displayed notable tissue-specific expression in testes. Notably, the SPATA3-I2 isoform protein was not expressed in embryos or during the early development stage of the mice, yet it was highly expressed in the testes of mice aged 23-57 days (3-8 weeks). Immunohistochemistry revealed that the SPATA3-I2 isoform protein was located mainly in round and elongated spermatids within the spermatogenic epithelial cells. In conclusion, the findings highlighted that SPATA3 isoforms had differential subcellular localizations and that SPATA3-I2 exhibited a specific spatiotemporal expression pattern, suggesting its association with spermatogenesis and sperm maturation.

Correspondence to: Dr Junjiang Fu, Key Laboratory of Epigenetics and Oncology, The Research Center for Preclinical Medicine, Southwest Medical University, 3-319 Zhongshan Road, Luzhou, Sichuan 646000, P.R. China
E-mail: fujunjiang@hotmail.com

Professor Qiang Wu, The State Key Laboratory of Quality Research in Chinese Medicine and Faculty of Chinese Medicine, Macau University of Science and Technology, Avenida Wai Long, Taipa, Macau SAR 999078, P.R. China
E-mail: qwu@must.edu.mo

*Contributed equally

Key words: spermatogenesis-associated protein 3, spermatogenesis, isoforms, subcellular localization, tissue-specific expression, male infertility

Introduction

According to the World Health Organization, infertility is defined as the inability to achieve a clinical pregnancy after ≥12 months of regular unprotected intercourse (1). This condition affects ~15% of reproductive-aged couples globally, with male factors contributing to ~50% of cases (2-4). Male infertility is characterized mainly by abnormal spermatogenesis and maturation, abnormal semen quality, chromosomal anomalies, Y chromosome microdeletions, congenital defects, and endocrine disorders (5-7). Spermatogenesis disorders are the most common cause of male infertility, resulting in azoospermia, oligozoospermia, asthenozoospermia, teratozoospermia or a combination of these conditions (8,9). The advance of assisted reproductive technologies, particularly intracytoplasmic sperm injection and microdissection testicular sperm extraction, has led to substantial progress in the diagnosis and treatment of male infertility (10-13). However, in-depth research into the molecular mechanisms of spermatogenesis is lacking, and the pathogenesis of male infertility remains poorly understood. Therefore, elucidating the expression patterns and subcellular localization, and identifying potential causative genes related to male infertility are crucial for investigating the pathogenesis of male infertility.

Mammalian spermatogenesis is a highly intricate and precisely regulated process that can be broadly categorized into three distinct stages. First, spermatogonial stem cells engage in self-renewal and proliferation through mitosis. Second, haploid

spermatids are formed via meiosis I/II. Third, haploid round spermatids undergo a transformation process (spermiogenesis) to form the complex structure of the mature spermatozoa (14). Gene expression regulation serves a crucial role in this process of germ cell differentiation throughout spermatogenesis. The development of advanced biotechniques, such as gene knockout and gene sequencing technologies, has substantially increased the ability to identify spermatogenesis-related genes. These include genes encoding spermatogenic cell cycle proteins, azoospermia factors, apoptosis-associated proteins, heat shock proteins, centrosomal proteins and cytoskeleton proteins (15-20). The regulation of spermatogenic apoptosis involves various factors, including the Bcl-2 family, the *p53* gene, the spermatogenesis-associated protein 3 (*SPATA3*) gene, the Fas/Fasl system, the mitochondrial ribosomal protein S22, the caspase family and the *C-myc* gene (21-25). Notably, the *SPATA3* gene is specifically expressed in the testis of both humans and mammals, and serves crucial roles in spermatogenesis and spermatogenic apoptosis (26,27). In humans, the *SPATA3* gene is located on chromosome 2q37.1 and exists in multiple isoforms (28). SPATA3 is conserved across mammals, evidenced by 55% identity between the mouse and human proteins (29). In mice, the *Spata3* gene encodes a basic, unstable, hydrophilic polypeptide. This protein lacks a signal peptide and is classified as a non-transmembrane intracellular protein (30). In 2003, through an integrated approach combining bioinformatics analysis and experimental techniques, Fu *et al* (26) successfully cloned the human testicular spermatogenic apoptosis-related gene *TSARG1* and its murine counterpart *Mtsarg1*, also known as *SPATA3* (GenBank no. NM_139073.3). This study pioneered the application of a mouse cryptorchidism model to postulate a close association between the *Spata3* gene and spermatogenic cell apoptosis during spermatogenesis. Subsequently, Li *et al* (31) cloned *Mtsarg1-β*, a mouse *Mtsarg1* gene transcript (GenBank accession nos. EU259321 and EF546784; named *Spata3* variant4), using mouse testicular cDNA as a template. This expanded the understanding of the genetic complexity associated with *Spata3* in mice. In 2018, Wang *et al* (32) reported that overexpression of the *Spata3* gene may be associated with spermatogonial autophagy during mammalian spermatogenesis. The authors also revealed the tissue-specific expression of Spata3 in mouse testicular tissue, highlighting its unique role in testicular function. In addition, in 2021, Girault *et al* (29) employed CRISPR/CRISPR associated protein 9 technology to knockout the *Spata3* gene in mice. These findings demonstrated that such knockout led to marked alterations in sperm morphology and a marked decrease in *in vitro* fertilization efficacy, thereby emphasizing the importance of this gene in sperm development and function. Malcher *et al* (27) demonstrated via gene microarray analysis that SPATA3 expression was markedly reduced in the testicular tissues of patients with nonobstructive azoospermia. Taken together, these findings demonstrated the crucial importance of the *SPATA3* gene in spermatogenesis. In our previous study, molecular cloning techniques revealed four distinct SPATA3 isoform sequences, designated as SPATA3-I1, SPATA3-I2, SPATA3-I3 and SPATA3-I4, with SPATA3-I3 and SPATA3-I4 representing two novel isoforms (28). Structural characterization demonstrated that SPATA3-I1 and SPATA3-I4 contain two repeats of the QQPSPESTP (PEST) domain, whereas SPATA3-I2 and SPATA3-I3 possess three repeats (28). Although SPATA3 serves an important role in cellular processes (29), such as autophagy and apoptosis regulation (26), the precise functional importance of these SPATA3 isoforms remains to be elucidated. To address this knowledge gap, the current investigation systematically examined both the expression patterns and subcellular localization of these isoforms during testicular development, aiming to elucidate their distinct roles in spermatogenesis regulation and male reproductive development.

Alternative splicing (AS) represents a sophisticated molecular process whereby a precursor messenger ribonucleic acid selectively splices specific exons together to generate a mature mRNA transcript (33). This resulting mRNA is translated into a diverse array of splicing isoforms. Isoforms encoded by the same gene can exhibit different biological functions and structural features (34). Furthermore, these genes may be expressed differently within the same cell or across different cellular compartments, giving rise to a spectrum of phenotypes (33). AS occurs in the transcription of ≥90% of human genes (35,36). This process substantially augments the diversity of protein structures and functions, and concurrently increases the complexity of gene expression (37,38). Therefore, AS serves as a pivotal mechanism for post-transcriptional gene expression regulation (37,39). Based on gene sequence analysis and microarray studies, AS is observed mainly in genes associated with tissues characterized by multiple cellular morphologies and complex functions, such as the brain and testis (20,40). Spermatogenesis is a highly regulated and intricate process, and an appropriate pattern of AS, along with stage-specific isoforms, is crucial for its successful progression (41). However, to date, in-depth investigations into AS and isoforms at different spermatogenic stages are limited (20,42). Notably, to the best of our knowledge, the function and subcellular localization of the SPATA3 isoforms have not yet been elucidated. Therefore, a comprehensive study of the biological properties and protein expression characteristics of SPATA3 variant splicing isoforms holds great promise. Such research can provide insights into the genomic structure, gene expression patterns, protein functions, and physiological and pathological mechanisms underlying spermatogenesis, thus providing a theoretical basis for the diagnosis and treatment of male infertility.

Based on previous research (28), the present study investigated the role, expression pattern and localization of SPATA3 isoforms using Cell Counting Kit-8 (CCK-8) assay, PCR, western blot analysis, immunohistochemistry, and other molecular and cell biology techniques. The spatiotemporal differences in the expression of SPATA3 isoforms were also analyzed. The present study is expected to lay a foundation for further studies on male infertility and the structure and function of the *SPATA3* gene.

Materials and methods

Animals. All animal experiments were performed as previously described (43), and adhered scrupulously to the animal care guidelines at international, national and institutional levels. The present study was reviewed and approved by the Ethics Committee of Southwest Medical University (approval

nos. 20160086 and 20210930-007; Luzhou, China). Briefly, a total of 9 BALB/c mice (3 male and 6 female mice; 5 weeks old; ~20 g) were purchased from SPF (Beijing) Biotechnology Co., ltd. The mice were individually housed at room temperature (range, 18-22˚C) with a relative humidity of 40-60%. They were maintained under a 12-h light/dark cycle. Mice had unrestricted access to food and water, available *ad libitum*. Multiple tissues of adult mice (including muscle, brain, heart, liver, spleen, lung, colon, kidney, breast, uterus, ovary and testis) were dissected. Tissues were immediately frozen in liquid nitrogen and stored at -80˚C until protein extraction for western blot analysis of SPATA3-I2 expression. In addition, testes were collected from Balb/c mice at 10 developmental stages (embryo, postnatal days 1, 13, 23, 30, 37, 47, 57, 67, and 83) to compare SPATA3-I2 expression in different developmental stages. For each stage, testes were obtained from 3 independent mice (n=3/group). The mice used in this study were derived from a breeding colony of BALB/c mice, including nine 5-week-old founders (3 males and 6 females) that served as the parental generation for producing offspring at each developmental stage. Euthanasia of the mice was achieved through intraperitoneal injection of pentobarbital sodium at a dose of 200 mg/kg of body weight. The confirmation of death was based on the absence of vital signs. This included the lack of a detectable heartbeat, the presence of dilated pupils and no response to cervical dislocation.

Cell culture. The HeLa cell line was obtained from American Type Culture Collection and cultured in DMEM/HIGH GLUCOSE (Thermo Fisher Scientific, Inc.). The culture medium was supplemented with 10% fetal bovine serum (Beijing Solarbio Science & Technology Co., Ltd.) and 1% penicillin-streptomycin (acquired from Beyotime Institute of Biotechnology). The cells were incubated at 37˚C in a 5% CO_2 incubator. Once the cell confluence reached 80%, the cells were washed twice with PBS. Subsequently, they were dissociated using trypsin (Beyotime Institute of Biotechnology) at 37˚C for 1.5 min to facilitate subculturing.

Plasmid and reagents. The pcDNA5/FRT/TO and pEGFP-C3 vector were purchased from Clontech Laboratories, Inc. The restriction enzymes *Eco*RI, *Eco*RV and *Bam*HI were obtained from Promega Corporation. Lipofectamine® 2000 was obtained from Invitrogen (Thermo Fisher Scientific, Inc.). Tubulin, Hsp90 and rabbit anti-SPATA3 antibodies were purchased from Proteintech Group, Inc., respectively. Hoechst 33258 staining solution was obtained from Beyotime Institute of Biotechnology. The CCK-8 was purchased from Shanghai Yeasen Biotechnology Co., Ltd. Reagent grade or higher was used for all chemicals and enzymatic reagents.

Bioinformatics analysis of the signal peptide and transmembrane regions of SPATA3 isoforms. For identification of the amino acid sequences of the SPATA3 isoforms, the National Center for Biotechnology Information database (ncbi.nlm.nih.gov/protein) was searched by entering '*SPATA3*'. The signal peptides of SPATA3-I1, SPATA3-I2, SPATA3-I3 and SPATA3-I4 (GenBank Accession nos. AY032925.1, AY032925.1, AYP71042.1 and AYP71043.1) were predicted using the online SignalP-6.0 server (https://services.healthtech.dtu.dk/services/SignalP-6.0/). The transmembrane region and the subcellular localization of SPATA3-I1, SPATA3-I2, SPATA3-I3 and SPATA3-I4 were predicted using the online TMHMM-2.0 tool (https://services.healthtech.dtu.dk/services/TMHMM-2.0/) and the WOLF PSORT tool (wolfpsort.hgc.jp/). The domains and other features of the SPATA3 isoforms were predicted using the online InterPro database (hwww.ebi.ac.uk/interpro/search/sequence/). In addition, the expression of the SPATA3 was predicted by The Human Protein Atlas (proteinatlas.org/) and Uniprot database (https://www.uniprot.org/).

Molecular cloning for AS variants of SPATA3 using the pcDNA5 and pEGFP-C3 vectors. In our previous study, the full-length cDNA of *SPATA3* was amplified using Human Testis Marathon-Ready cDNA library (Clontech (USA) as the template, and the full-length gene sequences of the open reading frames of the human open reading frame SPATA3 isoforms were obtained via cloning with the pGM-T vector (28). Using this plasmid as a template, amplify the full-length open reading frame sequences of SPATA3 isoforms via PCR. The expression vector pcDNA5 was double digested with *Eco*RV and *Bam*HI restriction enzymes, the expression vector pEGFP-C3 was double digested with *Eco*RI and *Bam*HI restriction enzymes, and the SPATA3 gene fragment was digested using the same restriction enzymes as the respective vectors and ligated into the digested backbones. Novel isoforms were cloned and inserted into the pcDNA5 plasmid (Clontech; Takara Bio USA, Inc.) to generate recombinant plasmids, which included pcDNA5-*SPATA3*-I1, pcDNA5-*SPATA3*-I2, pcDNA5-*SPATA3*-I3 and pcDNA5-*SPATA3*-I4. Similarly, novel isoforms were cloned and inserted into the plasmid pEGFP-C3 (Takara Bio USA, Inc.) to obtain recombinant plasmids, including pEGFP-C3-*SPATA3*-I1, pEGFP-C3-*SPATA3*-I2, pEGFP-C3-*SPATA3*-I3 and pEGFP-C3-*SPATA3*-I4. The amplification primers used are shown in Table I. Positive clones were verified by PCR amplification. Briefly, 0.5 μl single-colony culture medium was used as the template for SPATA3 isoform amplification, along with 1 μl of SPATA3 splicing variant-specific primers. The 10 μl PCR reaction system contained 5 μl of 2x Taq PCR Master Mix (Beyotime Bio Tech Co., Ltd) and 3.5 μl of ddH_2O. PCR amplification was performed using an Applied Biosystems Veriti® 96-Well Thermal Cycler (Life Technology, USA) with the following program: initial denaturation at 95˚C for 90 s; followed by 33 cycles of 94˚C for 40 s (denaturation), 64˚C for 30 s (annealing), and 72˚C for 40 s (extension); and a final extension at 72˚C for 3 min. The PCR products were separated by 1.8% agarose gel electrophoresis and stained with 0.5 μg/ml ethidium bromide (EB) for visualization. Densitometric analysis was conducted using a ChemiDoc XR system (version 5.2, Bio-Rad Laboratories, Inc.). Positive clones identified by PCR were further verified by Sanger sequencing on an ABI-3500DX sequencer (Applied Biosystems Inc., Foster City, CA, USA) (28).

Cell transfection. HeLa cells were transfected with 3 μl Lipofectamine® 2000 (Invitrogen; Thermo Fisher Scientific, Inc.) and 1 μg recombinant plasmid and/or empty vector. Subsequently, the cells were incubated in a humidified

Table I. Primers used for PCR amplification.

SPATA3 isoform	Primer name	Sequence (5'-3')	Vector
SPATA3-I1	*SPATA3*-5*Eco*RV	GTGGATATCATGAAGAAGGTCAAGAAGAAAA	pcDNA5
	SPATA3-3*Bam*HI	GTAGGATCCGTGATGTAGTAGGCAGCTCC	
SPATA3-I2	*SPATA3*-5*Eco*RV	GTGGATATCATGAAGAAGGTCAAGAAGAAAA	pcDNA5
	SPATA3-3*Bam*HI-S	GTGGGATCCTCACAAGGATTCAGTGATGTAGTAGGCAGCTCC	
SPATA3-I3	*SPATA3*-5*Eco*RV	GTGGATATCATGAAGAAGGTCAAGAAGAAAA	pcDNA5
	SPATA3-3*Bam*HI-S	GTGGGATCCTCACAAGGATTCAGTGATGTAGTAGGCAGCTCC	
SPATA3-I4	*SPATA3*-5*Eco*RV	GTGGATATCATGAAGAAGGTCAAGAAGAAAA	pcDNA5
	SPATA3-3*Bam*HI-S	GTGGGATCCTCACAAGGATTCAGTGATGTAGTAGGCAGCTCC	
SPATA3-I1	*SPATA3*-5*Eco*RI	GTGGAATTCTGAAGAAGGTCAAGAAGAAAAG	pEGFP-C3
	SPATA3-3*Bam*HI	GTGGGATCCTGATGTAGTAGGCAGCTCC	
SPATA3-I2	*SPATA3*-5*Eco*RI	GTGGAATTCTGAAGAAGGTCAAGAAGAAAAG	pEGFP-C3
	SPATA3-3*Bam*HI	GTGGGATCCTGATGTAGTAGGCAGCTCC	
SPATA3-I3	*SPATA3*-5*Eco*RI	GTGGAATTCTGAAGAAGGTCAAGAAGAAAAG	pEGFP-C3
	SPATA3-3*Bam*HI-S	GTGGGATCCTCACAAGGATTCAGTGATGTAGTAGGCAGCTCC	
SPATA3-I4	*SPATA3*-5*Eco*RI	GTGGAATTCTGAAGAAGGTCAAGAAGAAAAG	pEGFP-C3
	SPATA3-3*Bam*HI-S	GTGGGATCCTCACAAGGATTCAGTGATGTAGTAGGCAGCTCC	
	ACTB-F	CTCTTCCAGCCTTCCTTCCT	
	ACTB-R	CACCTTCACCGTTCCAGTTT	

SPATA3, spermatogenesis-associated protein 3; I, isoform. EcoRV, Escherichia coli Restriction Enzyme V. BamHI, Bacillus amyloliquefaciens H Restriction Enzyme I. Underlines indicate the portion of the sequence specific to SPATA3 for each primer.

atmosphere at 37˚C for 8 h. After transfection, the medium was replaced with fresh DMEM supplemented with 10% FBS. The cells were harvested 48 h post-transfection for analysis. The overexpression of mRNAs and proteins encoding SPATA3 isoforms was confirmed via reverse transcription (RT)-PCR and western blotting.

Cell proliferation analysis. After 48 h incubation, analysis of cell proliferation was performed using the CCK-8 assay (Shanghai Yeasen Biotechnology Co., Ltd.). Specifically, 10 μl CCK-8 reagent was added to each well containing 100 μl of culture medium, and plates were incubated at 37˚C in a 5% CO_2 incubator for 4 h. All procedures were conducted according to the manufacturer's instructions.

RT-PCR. Recombinant plasmids (pcDNA5-*SPATA3*-I1, pcDNA5-*SPATA3*-I2, pcDNA5-*SPATA3*-I3, pcDNA5-*SPATA3*-I4 and pEGFP-C3-SPATA3-I3) and the empty vector pcDNA5 were transfected into HeLa cells. Total RNA was extracted using an RNAsimple kit (Tiangen Biotech Co., Ltd.), and its quality was verified via agarose gel electrophoresis and UV spectrophotometry (A260/280=1.8-2.0). The first-strand cDNA was synthesized from 1 μg total RNA using the ReverTra Ace® qPCR RT kit (cat. no. FSQ-201; Toyobo Life Science) according to the manufacturer's protocol. Semi-quantitative RT-PCR was performed in a 10 μl reaction system containing 5 μl 2 x Taq PCR MasterMix (Tiangen Biotech Co.), 1 μl (2.5 μM) of each pair primer, 1 μl RT product, and 3 μl double-distilled H_2O. Amplification was carried out on an Applied Biosystems® Veriti® 96-Well Thermal Cycler (Thermo Fisher Scientific, Inc.) under the following conditions: Initial denaturation at 95˚C for 90 sec, followed by 33 cycles of 94˚C for 40 s, 60˚C for 30 s, and 68˚C for 40 s; followed by a final extension at 72˚C for 1 min. Primer sequences for SPATA3 isoforms and the ACTB internal control gene are detailed in Table I. PCR products were resolved in triplicate on 1% agarose gels and visualized by staining with 0.5 μg/ml ethidium bromide. Densitometric analysis was performed using a ChemiDoc XR system (version 5.2, Bio-Rad Laboratories, Inc.).

Western blot analysis. Recombinant plasmids (pcDNA5-*SPATA3*-I1, pcDNA5-*SPATA3*-I2, pcDNA5-*SPATA3*-I3 and pcDNA5-*SPATA3*-I4) and an empty vector were transfected into HeLa cells. Cells were lysed on ice using pre-chilled 1x EBC lysis buffer (20 mM Tris-HCl pH 8.0, 2 mM EDTA, 125 mM NaCl, 0.5% NP-40) supplemented with protease inhibitors (Roche, USA). Protein samples (~30 μg/lane), quantified by bicinchoninic acid assay, were separated by 10% SDS-PAGE and transferred to PVDF membranes. After being blocked with 5% nonfat milk in TBS with 0.1% Tween-20 for 2 h at room temperature, the membranes were incubated overnight at 4˚C with primary antibodies as follows: SPATA3 (1:2,000, cat. no. 17500-1-AP; Proteintech Group, Inc.), Flag (1:10,000, cat. no. F3165; Sigma-Aldrich, USA), Hsp90 (1:5,000, cat#: 13171-1-AP; Proteintech, China), and Tubulin (1:5,000, cat#: 66031-1-lg; Proteintech, China). After three TBST washes, membranes were incubated with HRP-conjugated secondary antibodies (both 1:5,000; goat anti-mouse, cat#: SA00001-1; goat anti-rabbit, cat. no. SA00001-2; both Proteintech Group, Inc.) for 2 h at room temperature. Signal detection and quantification were performed using Pierce™ ECL Western

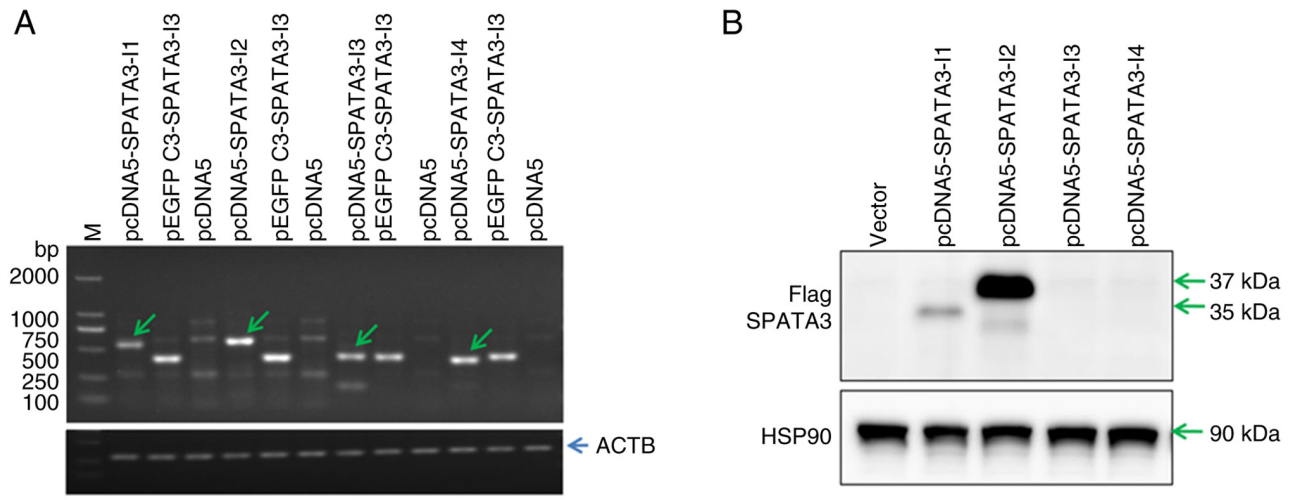

Figure 1. RT-PCR and western blotting results for SPATA3 isoform expression in HeLa cells transfected with pcDNA5 or pEGFP-C3 vectors containing SPATA3 isoforms. (A) RT-PCR analysis of SPATA3 isoform mRNA expression in HeLa transfected with pcDNA5 or pEGFP-C3 vectors containing SPATA3 isoforms. The green arrows indicate the expression of SPATA3-I1, SPATA3-I2, SPATA3-I3 and SPATA3-I4 mRNAs, and the corresponding fragment sizes are 552, 576, 418 and 418 bp, respectively. The pcDNA5 vector served as a negative control. ACTB served as an internal control. (B) Western blotting results of SPATA3 isoform protein expression in HeLa cells transfected with pcDNA5 vectors containing SPATA3 isoforms. Hsp90 served as an internal control. Vector, overexpression of the empty vector pcDNA5; RT-PCR, reverse transcription-PCR; SPATA3, spermatogenesis-associated protein 3; HSP90, heat shock protein 90.

Blotting Substrate (cat# 32106; Thermo Fisher Scientific, Inc.). The chemiluminescent signals were captured using a Gbox Chemi DRXV4/1068 chemiluminescence imaging system (Syngene, UK) and GENESYS software (Version V1.8.8.0, Syngene) (44).

Hoechst 33258 staining. HeLa cells were transfected with recombinant plasmids, specifically pEGFP-C3-*SPATA3*-I1, pEGFP-C3-*SPATA3*-I2, pEGFP-C3-*SPATA3*-I3 and pEGFP-C3-*SPATA3*-I4. After transfection, the cells were cultured for 24 h. The cells were subsequently stained with Hoechst 33258 and incubated at 37˚C in a humidified 5% CO_2 incubator for 30 min. Fluorescence imaging was performed using an Olympus IX81 fluorescence inverted microscope and CellSens Standard (V1.18, Olympus Corporation).

Immunohistochemical analysis. Testicular tissue from 2-, 8- and 16-week-old male mice were rapidly extracted after euthanasia, fixed with 4% paraformaldehyde in PBS at 4˚C for 24 h, and processed into 5 μm paraffin sections. Sections were deparaffinized, dehydrated, and subjected to antigen retrieval by microwave heating at 97˚C for 12 min in 10 mM citrate buffer (pH 6.0). After cooling, endogenous peroxidases were blocked with 3% H_2O_2 for 10 min at RT, followed by three PBS washes (5 min each). Nonspecific binding was blocked with 10% bovine serum albumin (cat#:A8020, Solarbio, China) at RT for 30 min, and sections were incubated overnight at 4˚C with rabbit anti-SPATA3 polyclonal antibody (cat#: 17500-1-AP; Proteintech, China; 1:50 in PBS). After washing, sections were incubated with HRP-conjugated goat anti-rabbit IgG secondary antibody (cat#: SA00001-2, Proteintech, China; 1:100 in PBS) for 1 h at RT in the dark, developed with DAB, counterstained with Mayer's hematoxylin at RT for 2 min, dehydrated through graded ethanol, cleared with xylene, mounted with Permount, and air-dried for light microscopy observation.

Statistical analysis. To evaluate the significance of differences between the experimental groups, the present study employed one-way ANOVA with Tukey's post hoc test for multiple comparisons. All statistical analyses were carried out using GraphPad Prism 9 (Dotmatics). Data are presented as mean ± standard deviation of two or three independent experimental repeats. $P<0.05$ was considered to indicate a statistically significant difference.

Results

Cloning and overexpression of SPATA3 isoforms. The four AS variants of SPATA3, namely SPATA3-I1, SPATA3-I2, SPATA3-I3 and SPATA3-I4, were successfully cloned and inserted into the pcDNA5 and pEGFP-C3 vectors. Sanger sequencing verified the results (data not shown). The RT-PCR results revealed the overexpression of SPATA3 mRNA isoforms (Fig. 1A). Furthermore, western blotting was performed to analyze the overexpression of SPATA3 isoforms in HeLa cells. The protein bands corresponding to pcDNA5-*SPATA3*-I1 and pcDNA5-*SPATA3*-I2 stably appeared, and the expression of pcDNA5-*SPATA3*-I2 was markedly greater (Fig. 1B). The signal intensities were normalized to Hsp90 as an internal control, Notably, this normalization yielded consistent ratios across repeated experiments, confirming the reliability of the results. Conversely, despite multiple attempts at cell transfection and western blotting, no visible bands corresponding to pcDNA5-*SPATA3*-I3 or pcDNA5-*SPATA3*-I4 were detected.

SPATA3 promotes cell proliferation in vitro. To explore the effect of SPATA3 on cell proliferation, the present study constructed the overexpression vectors pcDNA5-*SPATA3*-I1 and pcDNA5-*SPATA3*-I2. After HeLa cells were transfected with pcDNA5-*SPATA3*-I1, pcDNA5-*SPATA3*-I2 or the empty vector pcDNA5, a CCK-8 assay was used to detect cell

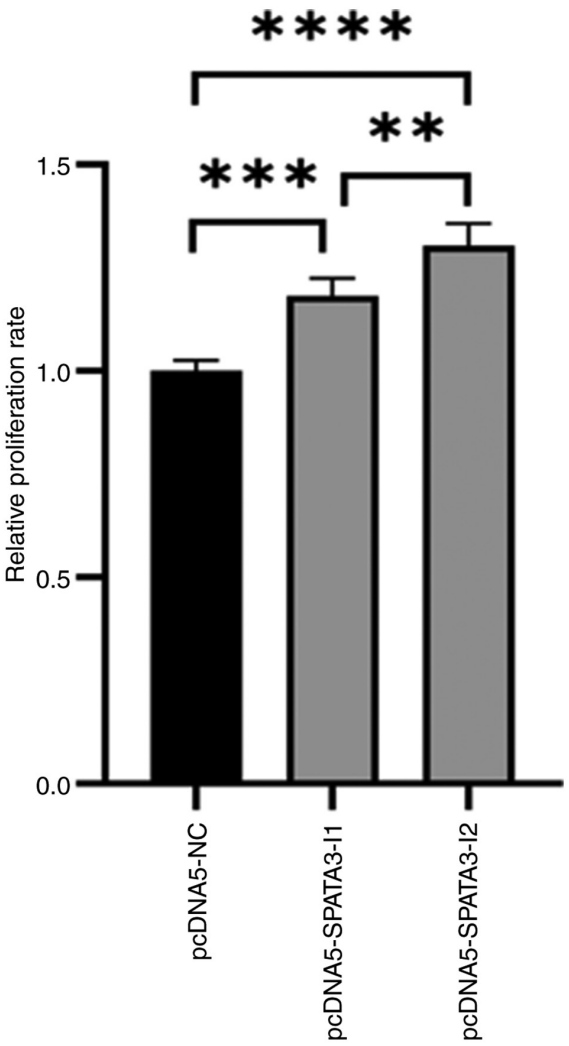

Figure 2. SPATA3 promotes HeLa cell proliferation *in vitro*. Relative proliferation rates of HeLa cells transfected with pcDNA5-SPATA3-I1, pcDNA5-SPATA3-I2 or the empty vector pcDNA5 at 48 h post-transfection. **P<0.01, ***P<0.001, ****P<0.0001. SPATA3, spermatogenesis-associated protein 3; NC, negative control.

proliferation at 48 h after transfection. The results revealed that, within 48 h, the overexpression of pcDNA5-*SPATA3*-I1 and pcDNA5-*SPATA3*-I2 led to a greater number of proliferating cells compared with that in the control group (Fig. 2). Notably, pcDNA5-SPATA3-I2 exhibited a more pronounced proliferative effect on HeLa cells than pcDNA5-SPATA3-I1. These findings indicated that SPATA3 promoted cell proliferation.

Signal peptides, transmembrane regions and features of SPATA3 isoforms. To predict the presence of signal peptides, transmembrane regions, subcellular localization and other features of SPATA3 isoforms, the present study utilized SignalP 6.0, TMHMM 2.0, WOLF PSORT and InterPro software. The results indicated that none of the SPATA3 isoforms harbored a signal peptide. Notably, only SPATA3-I3 and SPATA3-I4 possessed transmembrane regions (Fig. 3). Furthermore, according to the transmembrane topology prediction for SPATA3-I3 and SPATA3-I4 generated by TMHMM 2.0, SPATA3-I1 and SPATA3-I2 were predominantly located in the nucleus, whereas SPATA3-I3 and SPATA3-I4 were mainly distributed in both the nucleus and the cytoplasm. Additionally, the prediction results indicated that the SPATA3 family and the testis spermatocyte apoptosis-related gene 1 protein of SPATA3-I2 contained the longest amino acid sequence.

Subcellular localization of overexpressed SPATA3 isoforms. The subcellular localization of SPATA3 isoforms following overexpression of the pEGFP-C3 fusion protein in the aforementioned HeLa cells was determined. The results revealed distinct subcellular localization patterns for different SPATA3 isoform fusion proteins. Overexpression of pEGFP-C3-*SPATA3*-I1 and pEGFP-C3-*SPATA3*-I2 led to proteins predominantly localized in the nucleus (Fig. 4A-F, with almost 100% of the transfected cells showing predominantly nuclear fluorescence. Conversely, for the fusion proteins pEGFP-C3-*SPATA3*-I3 and pEGFP-C3-*SPATA3*-I4, as shown in Fig. 4G-L, higher fluorescence intensity was detected in the cytoplasm and lower intensity was detected in the nucleus. Specifically, ~87.5% of the cells transfected with pEGFP-C3-*SPATA3*-I3 presented predominantly cytoplasmic fluorescence, whereas nearly 100% of the cells transfected with pEGFP-C3-*SPATA3*-I4 presented the same cytoplasmic-predominant fluorescence pattern. The quantitative analysis of sub-cellular localization of different SPATA3 isoforms is shown in Fig. 4M.

SPATA3-I2 shows tissue-specific and spatiotemporal expression. Western blot analysis of SPATA3 protein expression in various tissues of BALB/c mice revealed that SPATA3-I2 was strongly present in the testis (Fig. 5A and B). In terms of SPATA3 protein expression in the testicular tissue of BALB/c mice at different developmental stages, the results revealed that the SPATA3-I2 protein was highly expressed in the testes of adult mice. Specifically, it was highly expressed in the testes of mice aged 23-57 days, whereas its expression was low in the testes of 83-day-old mice. Furthermore, low expression of SPATA3-I2 was detected in the testes of embryonic and 1-day-old mice (Fig. 5C and D). These findings suggested that SPATA3 may serve a crucial role in male development and spermatogenesis.

Subcellular localization of SPATA3 in round spermatids and elongated spermatids of mouse testes. Immunohistochemical results for SPATA3 in the testes of BALB/c mice revealed that the SPATA3 protein was undetectable in spermatogonia, pachytene spermatocytes, Leydig cells or mature sperm. Notably, intense fluorescence staining of SPATA3 was observed in both round spermatids and elongated spermatids. This observation indicated prominent stage-specific expression of SPATA3 (Fig. 6).

Discussion

In mammals, spermatogenesis is a complex process of germ cell differentiation that encompasses the mitosis, meiosis and sperm morphogenesis stages (14,45). Meiosis and morphogenesis exhibit differentiation phenomena that are not found in other cells, such as spermatid elongation and acrosome formation (46). The process of spermatogenesis is

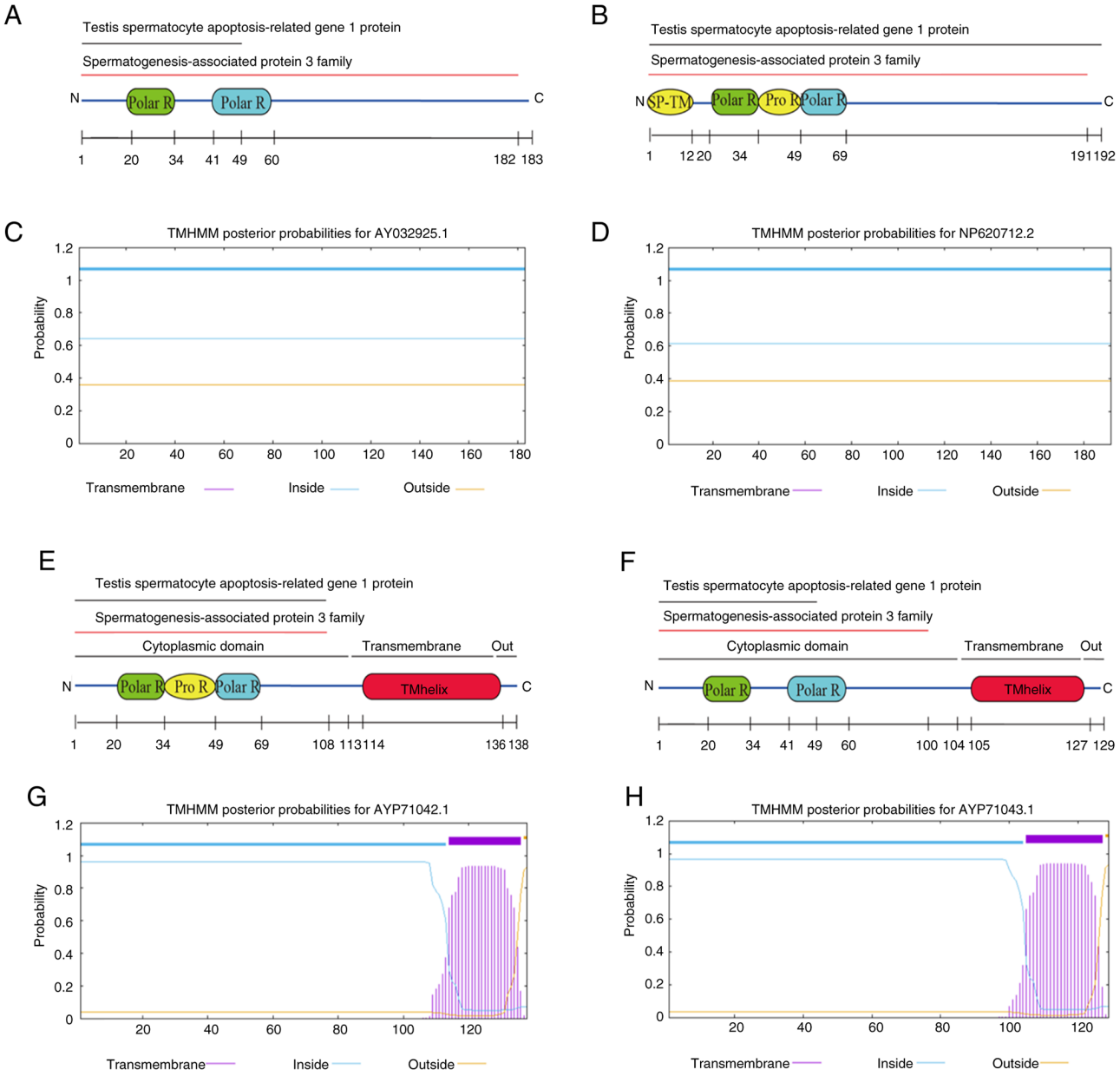

Figure 3. Domains, families and other features of SPATA3 isoforms. Schematic representation of domains, families and features in (A) SPATA3-I1. (B) Schematic representation of domains, families, and features in SPATA3-I2. (C) Transmembrane topology prediction for SPATA3-I1 generated by TMHMM 2.0. (D) Transmembrane topology prediction for SPATA3-I2 generated by TMHMM 2.0. (E) Schematic representation of domains, families, and features in SPATA3-I3. (F) Schematic representation of domains, families, and features in SPATA3-I4. (G) Transmembrane topology prediction for SPATA3-I3 generated by TMHMM 2.0. (H) Transmembrane topology prediction for SPATA3-I4 generated by TMHMM 2.0. SPATA3, spermatogenesis-associated protein 3; Polar R, polar residues; Pro R, pro residues; SP-TM, SignalP-TM; TMhelix, Transmembrane Helix.

precisely regulated by hundreds of genes (47,48). However, the expression, localization, function and regulatory mechanism of numerous genes involved in this process are not yet clear. It has been reported that SPATA3 serves a crucial role in spermatogenesis in mammals (26-29). In mice, deletion of SPATA3 induced morphological alterations in sperm and *in vitro* hypofertility, demonstrating its essential role in sperm maturation (29). In humans, SPATA3 was identified as a potential biomarker for nonobstructive azoospermia, with markedly reduced expression in testicular biopsies of affected individuals (27). Additionally, molecular studies in mice revealed that Mtsarg1 (a homolog of human SPATA3) is dynamically expressed during spermatogenesis and may regulate germ cell apoptosis (26,31). Therefore, it is important to study the physiological mechanism of the SPATA3 related to spermatogenesis, as well as the pathological mechanism of spermatogenesis disorders. The present study investigated the role of SPATA3 in cell proliferation, as well as the expression pattern and localization of its various splicing isoforms in testicular tissues, and analyzed the spatiotemporal expression and function of SPATA3.

RT-PCR analysis confirmed the successful induction of overexpression for distinct SPATA3 isoform overexpression. However, the subsequent western blotting results from multiple repeated experiments revealed that specific bands were observed only for the expression of pcDNA5-*SPATA3*-I1 and

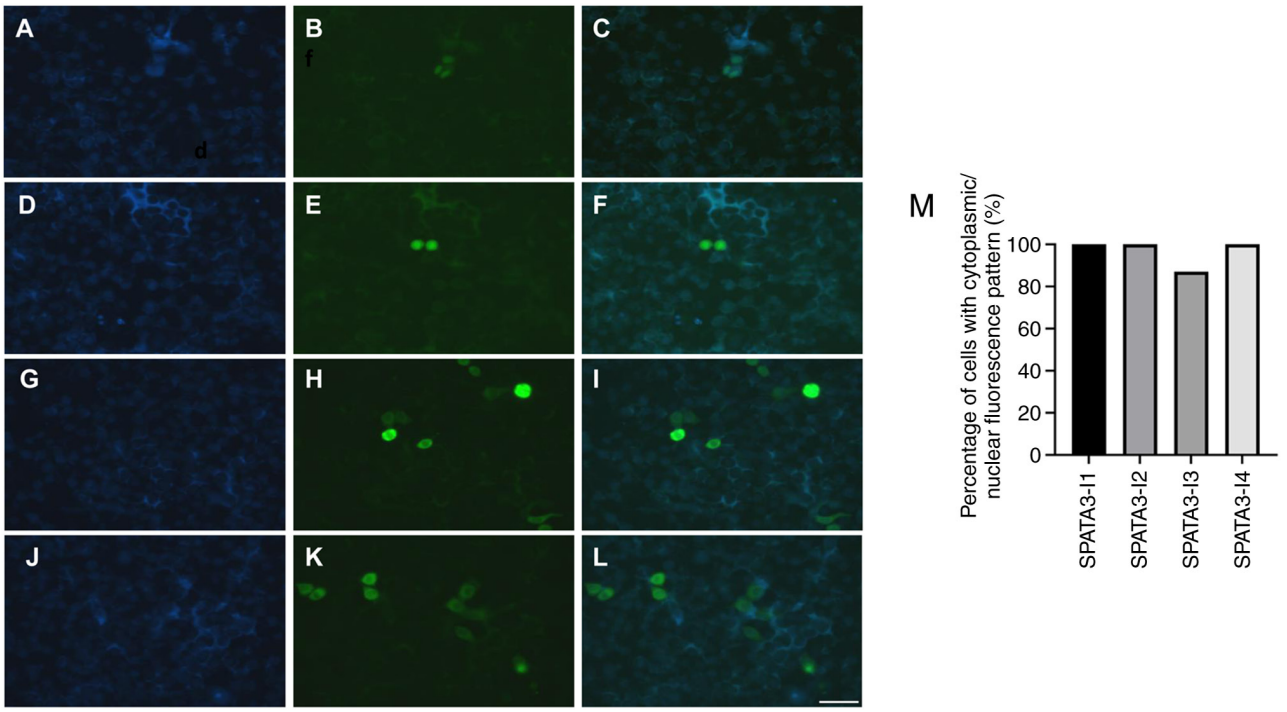

Figure 4. Subcellular localization of overexpressed SPATA3 isoforms in HeLa cells. Cells overexpressing the pEGFP-C3-SPATA3-I1 isoform. (A) Hoechst 33258 staining. (B) GFP signals for overexpression of pEGFP-C3-SPATA3-I1 isoform; (C) Merged images of Hoechst 33258 staining and GFP signals. Cells overexpressing the pEGFP-C3-SPATA3-I2 isoform. (D) Hoechst 33258 staining; (E) GFP signals for overexpression of pEGFP-C3-SPATA3-I2 isoform; (F) Merged images of Hoechst 33258 staining and GFP signals. (G-I) Cells overexpressing the pEGFP-C3-SPATA3-I3 isoform. (G) Hoechst 33258 staining; (H) GFP signals for overexpression of pEGFP-C3-SPATA3-I3 isoform; (I) Merged images of Hoechst 33258 staining and GFP signals. (J-L) Cells overexpressing the pEGFP-C3-SPATA3-I4 isoform. (J) Hoechst 33258 staining; (K) GFP signals for overexpression of pEGFP-C3-SPATA3-I4 isoform; (L) Merged images of Hoechst 33258 staining and GFP signals. Scale bar, 50 μm. (M) Quantitative analysis of the sub-cellular localization of different SPATA3 isoforms. SPATA3, spermatogenesis-associated protein 3.

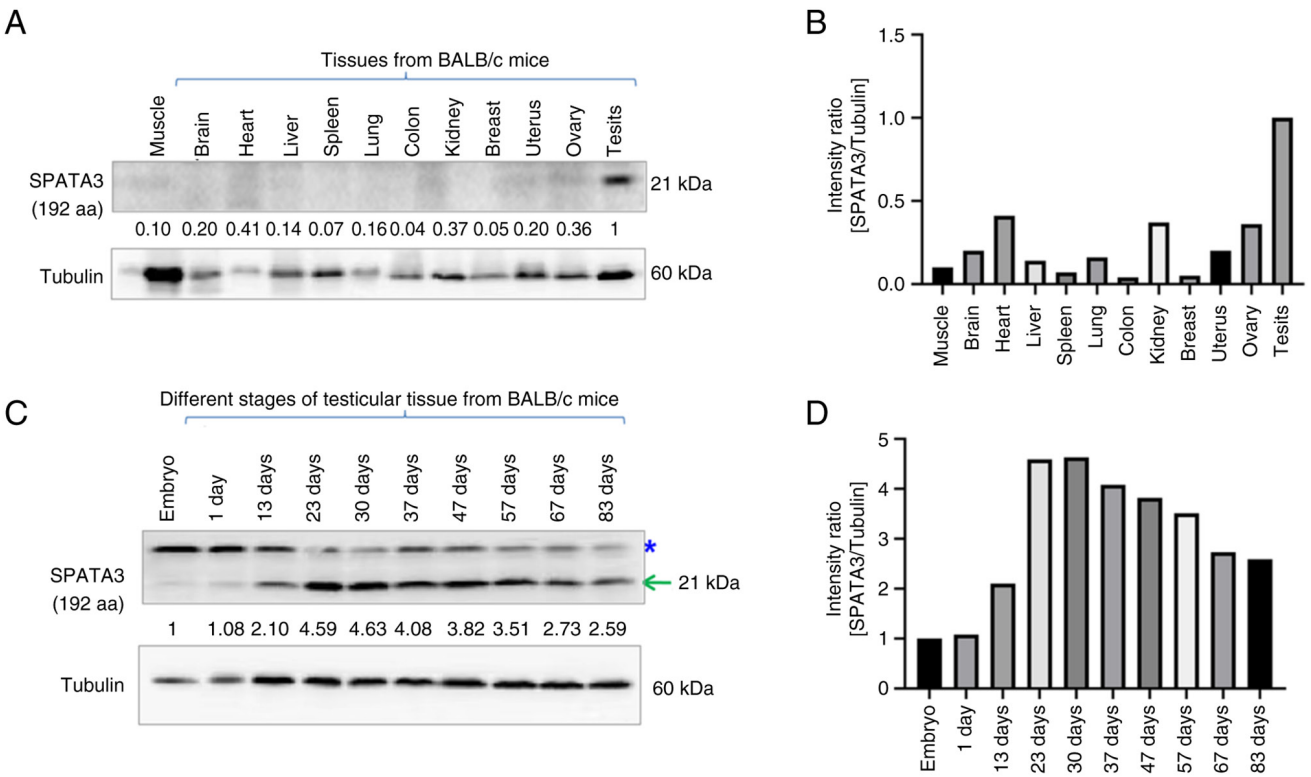

Figure 5. Western blot analysis of tissue-specific and stage-specific SPATA3 protein expression. (A) SPATA3 protein expression in various tissues of BALB/c mice and (B) semi-quantitative analysis. (C) SPATA3 protein expression in the testicular tissue of BALB/c mice at different developmental stages and (D) the associated semi-quantitative analysis. The arrow indicates the SPATA3 protein. The asterisk indicates nonspecific bands. SPATA3, spermatogenesis-associated protein 3.

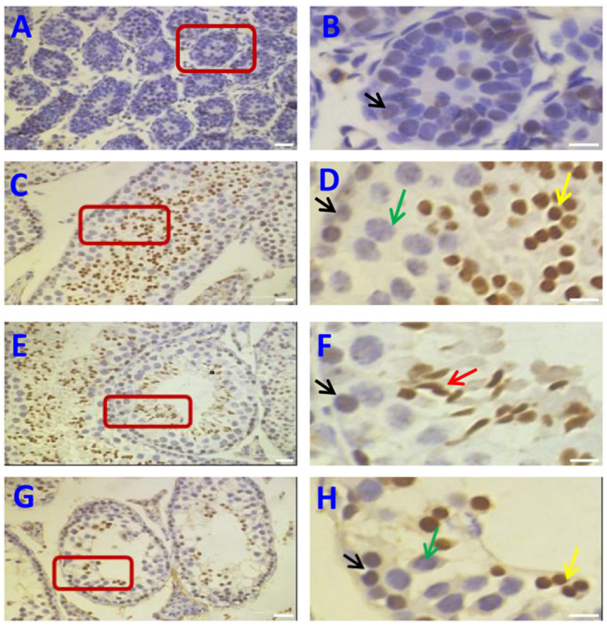

Figure 6. Immunohistochemistry results of spermatogenesis-associated protein 3 in the testes of BALB/c mice. (A) General expression pattern in the testicular tissue of 2 - week - old mice. (B) The images show a higher magnification of an area within red boxes in the left images. (C) The images show a general expression pattern in the testicular tissue of 8 - week - old mice. (D) The images show a higher magnification of an area within red boxes in the left images. (E) The images show a general expression pattern in the testicular tissue of 8 - week - old mice. (F) The images show a higher magnification of an area within red boxes in the left images. (G) The images show a general expression pattern in the testicular tissue of 19 - week - old mice. (H) The images show a higher magnification of an area within red boxes in the left images. The black arrows indicate spermatogonia, the green arrows indicate spermatocytes, the yellow arrows indicate round spermatids and the red arrow indicates elongated spermatids. Scale bar, 50 μm. (B, D, F and H) Scale bar, 20 μm.

pcDNA5-*SPATA3*-I2. These results provided tentative support for the hypothesis that these two proteins may exhibit relatively high stability. The stable band signals indicate that within the cell, the proteins encoded by pcDNA5-*SPATA3*-I1 and pcDNA5-*SPATA3*-I2 may resist the action of various intracellular degradation mechanisms and exist at relatively stable levels. With respect to pcDNA5-*SPATA3*-I3 and pcDNA5-*SPATA3*-I4, although various optimization measures were used to improve the sensitivity of western blotting detection, no corresponding bands were detected. Given that all the isoforms were subjected to the same experimental conditions during sample preparation and western blot analysis, the absence of these bands is likely due to protein degradation. If these proteins were stably present, according to the normal western blotting detection principle, bands similar to those of pcDNA5-*SPATA3*-I1 and pcDNA5-*SPATA3*-I2 should have been observable. Therefore, it was hypothesized that the proteins encoded by pcDNA5-*SPATA3*-I3 and pcDNA5-*SPATA3*-I4 either were not translated into polypeptides or were subjected to degradation processes. As a result, these proteins were undetectable via western blot analysis. It was hypothesized that the difference in the subcellular localization of the SPATA3 isoforms may be associated with degradation of the proteins outside of the nucleus. The speculation that protein is degraded outside the nucleus is based on several biological principles (49). Different subcellular locations can expose proteins to distinct cellular environments. In the case of SPATA3 isoforms, those not localized within the nucleus are likely to encounter a different set of proteolytic enzymes and regulatory factors in the cytoplasm or other extra-nuclear compartments (49). For example, the cytoplasm contains various proteasomal and lysosomal systems that are responsible for protein degradation (49). This may lead to a decrease in the levels of the extranuclear SPATA3 isoforms and nuclear proteins could be shielded from these systems or stabilized by nuclear binding partners, which in turn might be associated with differences in their subcellular localization patterns (50). Additionally, the amino acid sequences of the SPATA3-I1 and SPATA3-I2 isoforms may contain functional domains that affect the stability of the proteins. SPATA3-I1 consists of 549 bases, encoding a protein of 183 amino acids. SPATA3-I2 has 576 bases, and its translated protein contains 192 amino acids. These two isoforms are highly identical, with only seven amino acids missing at the N-terminus in SPATA3-I2. On the other hand, SPATA3-I3 is composed of 414 bases, encoding a 138-amino-acid protein, and SPATA3-I4 has 387 bases, with a translated protein of 129 amino acids. Compared with SPATA3-I1 and SPATA3-I2, SPATA3-I3 and SPATA3-I4 have more C-terminus deletions. The absence of these amino acid sequences in SPATA3-I3 and SPATA3-I4 likely leads to the loss of certain functional domains that are present in SPATA3-I1 and SPATA3-I2 (28). Taken together, these findings indicated a potential association between the stability of the proteins and the absence of amino acid sequences in SPATA3-I3 and SPATA3-I4. Nevertheless, the present study is that it did not employ proteasome inhibitor treatment to investigate the proposed stability differences among the SPATA3 isoforms, particularly regarding the hypothesis that SPATA3-I3 and SPATA3-I4 might be more easily degraded. Future research should incorporate proteasome inhibitor assays to precisely assess the role of the proteasomal degradation pathway in regulating the stability of different SPATA3 isoforms.

Spermatogenesis is a continuous process of cell differentiation. Romeo-Cardeillac *et al* (38) detected a high number of alternative gene splicing variants, which were observed in mouse purified, stage-restricted testicular cell populations, during different spermatogenic stages. These findings suggest that appropriate AS patterns and stage-specific isoforms are essential for successful spermatogenesis. In the present study, the SPATA3-I1 and SPATA3-I2 isoforms corresponded to cDNAs containing exons 1, 2 and 3, whereas SPATA3-I3 and SPATA3-I4 corresponded to cDNAs with exons 1 and 3, where exon 2 was skipped. Furthermore, a notable difference exists between SPATA3-I1/SPATA3-I2 and SPATA3-I3/SPATA3-I4, namely a 27-nt motif encoding a 9-AA peptide (28). SPATA3-I1 and SPATA3-I4 have two repeats of the PEST domain, while SPATA3-I2 and SPATA3-I3 have three repeats. The different numbers of PEST domain repeats may influence their ability to interact with nuclear transport-related proteins. Since SPATA3 is mainly expressed in the testis and is involved in spermatogenesis, these isoforms may participate in regulating gene expression in the nucleus, perhaps by interacting with transcription factors or chromatin-associated proteins (28). SPATA3-I3 and SPATA3-I4, with their relatively shorter protein lengths due to exon skipping, may be more likely to

be retained in the cytoplasm (28), which is consistent with the present findings regarding the subcellular localization of overexpressed SPATA3 isoforms. Their putative role in the cytoplasm may be associated with post-translational regulation during spermatogenesis. They may interact with cytoplasmic proteins involved in sperm cell development, such as proteins related to cytoskeletal organization, protein trafficking or signal transduction pathways that are crucial for the proper formation and maturation of sperm cells. Although splice acceptor sites serve a vital role in this process, the splicing mechanism may not adhere strictly to a fixed rule (20,51,52). Therefore, there are four alternatively spliced isoforms, which either include or exclude exon 2 and feature 2-3 repeats in the conserved domain (28,29). Nevertheless, the functions of different isoforms in regulating spermatogenesis and their participation in the pathological mechanisms of male infertility remain to be elucidated. Research on the alterations of these isoforms during spermatogenesis could offer a novel perspective for uncovering causes of male infertility.

To the best of our knowledge, there have been no reports on the effects of diverse SPATA3 isoforms on cell proliferation. The present study investigated the effects of overexpression of SPATA3-I1 and SPATA3-I2 on the proliferation of HeLa cells. CCK-8 analysis revealed that, compared with SPATA3-I1, SPATA3-I2 had more pronounced proliferative effects on HeLa cells. This finding showed a positive association with the length of protein products encoded by the open reading frames of each isoform. The longer translation product might indicate a more complete structure, suggesting that different SPATA3 isoforms could have distinct functions. It has been reported that the *SPATA3* gene is one of the most markedly downregulated genes in the testes of infertile men diagnosed with nonobstructive azoospermia, demonstrating that *SPATA3* serves an important role in spermatogenesis (27). This finding is consistent with the present study. The present study further revealed that the overexpression of SPATA3-I1 and SPATA3-I2 markedly promoted the proliferation of HeLa cells. However, the underlying molecular mechanisms of this complex action remain unclear, necessitating further investigation to elucidate this phenomenon.

In the present study, the recombinant plasmids pEGFP-C3-*SPATA3*-I1, pEGFP-C3-*SPATA3*-I2, pEGFP-C3-*SPATA3*-I3 and pEGFP-C3-*SPATA3*-I4 were successfully constructed. These plasmids were validated by DNA sequencing and subsequently transfected into HeLa cells. At 24 h after transfection, nuclear staining with Hoechst 33258 revealed that the fusion proteins pEGFP-C3-*SPATA3*-I1 and pEGFP-C3-*SPATA3*-I2 were predominantly located in the nucleus, whereas pEGFP-C3-*SPATA3*-I3 and pEGFP-C3-*SPATA3*-I4 were mainly localized in the nucleus and the cytoplasm. These results were consistent with the predictions made by the online WOLF PSORT system. The subcellular localization of target proteins is determined by multiple factors, including the nuclear localization sequence, the hydrophobic signal peptide at the N-terminus of extracellular proteins and the internal hydrophobic structural domains of transmembrane proteins (53). The present study indicated that none of the SPATA3 isoforms contained a signal peptide, whereas only SPATA3-I3 and SPATA3-I4 possessed a transmembrane region. In addition, western blot and subcellular localization data suggested that the green fluorescent protein fusion proteins pEGFP-C3-*SPATA3*-I3 and pEGFP-C3-*SPATA3*-I4 were more stable than the proteins pcDNA5-*SPATA3*-I3 and pcDNA5-*SPATA3*-I4. Therefore, to further elucidate the functions of the SPATA3 isoforms in spermatogenesis, it is essential to conduct a comprehensive analysis of their structural domains, post-translational modifications and other underlying mechanisms.

On the basis of the 55% amino acid identity and 61% similarity between the mouse *spata3* and human *SPATA3* genes (26), the present study used mouse models to verify the expression of the SPATA3 protein. The present study focused on SPATA3-I2 isoform (RefSeq NM_001206998) for several reasons. Transcriptomic and proteomic data imply that SPATA3-I2 is the predominant isoform in human testis (28). Furthermore, InterPro predictions show that it has the longest amino acid sequence among SPATA3 isoforms.

Among the cloned isoforms, SPATA3-I2 is well-characterized in spermatogenesis. It has a more conserved structure, with species-conserved key domains potentially regulating sperm development (28). The western blotting results revealed that the SPATA3-I2 protein was specifically expressed in mouse testicular tissues, with high expression levels in mature testes and reduced or absent expression in aged and juvenile testes. This finding indicated a stage-specific difference in the expression of the SPATA3-I2 protein in mouse testes, which is consistent with the bioinformatics predictions from The Human Protein Atlas and Uniprot. Notably, a nonspecific band with a mirror-like pattern was observed. On the one hand, the nonspecific band might result from a cross-reaction of the antibody (54). However, during sample preparation, measures were taken, such as adding protease inhibitors and maintaining consistent processing conditions for all samples, to minimize this likelihood. On the other hand, it was hypothesized that the nonspecific band might be an additional isoform with a relatively high molecular weight. For example, one reported isoform of the protein uses an additional upstream exon, skipping exon 1 during splicing to generate a 355-amino acid variant, which differs from the canonical form (55). This hypothesis will be explored in more depth in future studies. Additionally, the immunohistochemical results demonstrated that the SPATA3-I2 protein was expressed mainly in round and elongated spermatids. Specifically, the nucleus of a round spermatid undergoes flattening and elongation, coupled with chromatin condensation, during the elongation phase of spermiogenesis. These structural modifications are crucial for the proper packaging of genetic material and the formation of a streamlined sperm head, which ensures optimal sperm motility and fertilization efficiency (56). The strong fluorescence staining of SPATA3 that was observed in both round spermatids and elongated spermatids indicated that SPATA3-I2 served roles in spermatogenesis and sperm maturation, such as regulating sperm metamorphosis and nuclear enrichment. During mammalian spermiogenesis, round spermatids undergo a series of biochemical and morphological changes to form elongated spermatids (45,57), followed by the development of testicular spermatozoa. During this process, the arrest of round spermatid differentiation is associated with the termination of spermatogonial development at a later stage of metamorphosis, which is characterized by substantial apoptosis (58-60). The mechanism of sperm metamorphosis is complex and is regulated by multiple genes (61-63). To gain a deeper understanding of

the mechanism of spermatogenesis, it is essential to clarify the regulatory mechanism of SPATA3-I2 in spermatogenesis and sperm maturation. Fu *et al* (26) first utilized a mouse cryptorchidism model to hypothesize that this gene is associated with the apoptosis of spermatogenic cells during spermatogenesis. Later, Wang *et al* (32) reported that the overexpression of SPATA3 may be closely related to the autophagy of spermatogenic cells during spermatogenesis in mammals. These researchers also confirmed the specific expression of SPATA3 in the testicular tissue of mice. As proposed by Anbazhagan *et al* (64), the binding of SPATA3 to Kelch-like family member 10 may promote the ubiquitination of related proteins, which function in the later stages of spermatogenesis. Furthermore, its expression is closely linked to the mRNA-microRNA (miRNA/miR) network, with miRNAs such as miR-26a potentially regulating it (56). Future studies should prioritize elucidating the molecular interplay between SPATA3 and spermatogenesis-associated proteins/pathways, leveraging advanced techniques such as co-immunoprecipitation, CRISPR-based functional screens or single-cell transcriptomics to map its regulatory network and downstream targets. Overall, while the current results provided valuable insights into the expression pattern of SPATA3-I2, further research is needed to fully understand its complex role in spermatogenesis and sperm maturation at the molecular level. In addition, although SPATA3-I2 seems pivotal for sperm maturation, the potential functions of alternative isoforms such as SPATA3-I1, SPATA3-I3 and SPATA3-I4 in spermatogenesis have yet to be investigated. Future research should determine whether these variants operate in a cooperative manner or display stage-specific expression patterns.

The present study demonstrated the expression of diverse SPATA3 isoforms, each with distinct subcellular localizations, and elucidated the role of SPATA3 in cell proliferation. SPATA3-I2 displayed a tissue-specific expression profile in testes and was closely associated with spermatogenesis, particularly sperm maturation. The present study provided a theoretical basis for clarifying the physiological and pathological mechanisms underlying spermatogenesis. The present study could be valuable for investigations into male infertility treatment strategies and contraceptive methods.

Acknowledgements

Not applicable.

Funding

The present study was supported by the National Natural Science Foundation of China (grant no. 30371493), the National Natural Science Foundation of China (grant nos. 81672887 and 82073263) and the Foundation of Science and Technology Department of Sichuan Province (grant no. 2022NSFSC0737). QW is funded by The Science and Technology Development Fund, Macau SAR [file no. SKL-QRCM (MUST)-2023-2025].

Availability of data and materials

The data generated in the present study may be requested from the corresponding author.

Authors' contributions

JF and QW designed and supervised the project. BZ, LF, JC and XJ conducted the experiments. LF and JF wrote the draft manuscript. LF, QW and JF edited the manuscript. All authors have read and approved the final version of the manuscript. JF and BZ confirm the authenticity of all the raw data.

Ethics approval and consent to participate

The animal experiments were approved by the Ethics Committee of Southwest Medical University (ethics approval nos. 20160086 and 20210930-007; Luzhou, China).

Patient consent for publication

Not applicable.

Competing interests

The authors declare that they have no competing interests.

References

1. Rowe PJ, Comhaire FH, Hargreave B and Mahmoud AMA (eds): WHO Manual for the Standardized Investigation, Diagnosis and Management of the Infertile Male. Cambridge University Press, Cambridge, UK, pp91, 2000.
2. Minhas S, Bettocchi C, Boeri L, Capogrosso P, Carvalho J, Cilesiz NC, Cocci A, Corona G, Dimitropoulos K, Gül M, *et al*: European association of urology guidelines on male sexual and reproductive health: 2021 update on male infertility. Eur Urol 80: 603-620, 2021.
3. Agarwal A, Baskaran S, Parekh N, Cho CL, Henkel R, Vij S, Arafa M, Panner Selvam MK and Shah R: Male infertility. Lancet 397: 319-333, 2021.
4. Fu L, Wu Q and Fu J: Exploring the biological roles of DHX36, a DNA/RNA G-quadruplex helicase, highlights functions in male infertility: A comprehensive review. Int J Biol Macromol 268 (Pt 2): 131811, 2024.
5. Eisenberg ML, Esteves SC, Lamb DJ, Hotaling JM, Giwercman A, Hwang K and Cheng YS: Male infertility. Nat Rev Dis Primers 9: 49, 2023.
6. Fu J, Li L and Lu G: Relationship between microdeletion on Y chromosome and patients with idiopathic azoospermia and severe oligozoospermia in the Chinese. Chin Med J (Engl) 115: 72-75, 2002.
7. Fu L, Xiong DK, Ding XP, Li C, Zhang LY, Ding M, Nie SS and Quan Q: Genetic screening for chromosomal abnormalities and Y chromosome microdeletions in Chinese infertile men. J Assist Reprod Genet 29: 521-527, 2012.
8. Kuroda S, Usui K, Sanjo H, Takeshima T, Kawahara T, Uemura H and Yumura Y: Genetic disorders and male infertility. Reprod Med Biol 19: 314-322, 2020.
9. Tüttelmann F, Ruckert C and Röpke A: Disorders of spermatogenesis: Perspectives for novel genetic diagnostics after 20 years of unchanged routine. Med Genet 30: 12-20, 2018.
10. Gül M, Russo GI, Kandil H, Boitrelle F, Saleh R, Chung E, Kavoussi P, Mostafa T, Shah R and Agarwal A: Male infertility: New developments, current challenges, and future directions. World J Mens Health 42: 502-517, 2024.
11. Wang Y, Li R, Yang R, Zheng D, Zeng L, Lian Y, Zhu Y, Zhao J, Liang X, Li W, *et al*: Intracytoplasmic sperm injection versus conventional in-vitro fertilisation for couples with infertility with non-severe male factor: A multicentre, open-label, randomised controlled trial. Lancet 403: 924-934, 2024.
12. Palermo G, Joris H, Devroey P and Van Steirteghem AC: Pregnancies after intracytoplasmic injection of single spermatozoon into an oocyte. Lancet 340: 17-18, 1992.
13. Schlegel PN: Testicular sperm extraction: Microdissection improves sperm yield with minimal tissue excision. Hum Reprod 14: 131-135, 1999.

14. Griswold MD: Spermatogenesis: The commitment to meiosis. Physiol Rev 96: 1-17, 2016.
15. Zhu X, Hu K, Cheng H, Wu H, Li K, Gao Y, Lv M, Xu C, Geng H, Shen Q, *et al*: Novel MEIOB pathogenic variants including a homozygous non-canonical splicing variant, cause meiotic arrest and human non-obstructive azoospermia. Clin Genet 105: 99-105, 2024.
16. Lee TH, Song SH, Kim DK, Shim SH, Jeong D and Kim DS: An analysis of Y-chromosome microdeletion in infertile Korean men with severe oligozoospermia or azoospermia. Investig Clin Urol 65: 77-83, 2024.
17. Tsai-Morris CH, Sheng Y, Lee E, Lei KJ and Dufau ML: Gonadotropin-regulated testicular RNA helicase (GRTH/Ddx25) is essential for spermatid development and completion of spermatogenesis. Proc Natl Acad Sci USA 101: 6373-6378, 2004.
18. Liman N: Heat shock proteins are differentially expressed in the domestic cat (Felis catus) testis, epididymis, and vas deferens. Microsc Microanal 29: 713-738, 2023.
19. Zhang X, Wang L, Ma Y, Wang Y, Liu H, Liu M, Qin L, Li J, Jiang C, Zhang X, *et al*: CEP128 is involved in spermatogenesis in humans and mice. Nat Commun 13: 1395, 2022.
20. Song H, Wang L, Chen D and Li F: The function of Pre-mRNA alternative splicing in mammal spermatogenesis. Int J Biol Sci 16: 38-48, 2020.
21. Yan W, Suominen J, Samson M, Jégou B and Toppari J: Involvement of Bcl-2 family proteins in germ cell apoptosis during testicular development in the rat and pro-survival effect of stem cell factor on germ cells in vitro. Mol Cell Endocrinol 165: 115-129, 2000.
22. Xiao B, Li X, Feng XY, Gong S, Li ZB, Zhang J, Yuan HJ and Tan JH: Restraint stress of male mice induces apoptosis in spermatozoa and spermatogenic cells: role of the FasL/Fas system†. Biol Reprod 101: 235-247, 2019.
23. Li YQ, He QH, Zhou Q, Zhou X, Bin DH, Liu CS and Guo JH: Impact of Ureaplasma urealyticum infection on the MRPS22 protein expression in rat spermatogenic cells and intervening effect of Zhibai Dihuang Decoction. Zhonghua Nan Ke Xue 25: 55-61, 2019 (In Chinese).
24. Feng Y, Shi J, Li M, Duan H and Shao B: Evaluation of the cytotoxic activity of triphenyl phosphate on mouse spermatocytes cells. Toxicol In Vitro 90: 105607, 2023.
25. Turunen HT, Sipilä P, Strauss L, Björkgren I, Huhtaniemi I and Poutanen M: Loss of Bmyc results in increased apoptosis associated with upregulation of Myc expression in juvenile murine testis. Reproduction 144: 495-503, 2012.
26. Fu JJ, Lu GX, Li LY, Liu G, Xing XW and Liu SF: Molecular cloning for testis spermatogenesis cell apoptosis related gene TSARG1 and Mtsarg1 and expression analysis for Mtsarg1 gene. Yi Chuan Xue Bao 30: 25-29, 2003 (In Chinese).
27. Malcher A, Rozwadowska N, Stokowy T, Kolanowski T, Jedrzejczak P, Zietkowiak W and Kurpisz M: Potential biomarkers of nonobstructive azoospermia identified in microarray gene expression analysis. Fertil Steril 100: 1686-1694.e1-7, 2013.
28. Zhou B, Wei C, Khan MA, Chen H and Fu J: Characterization and molecular cloning of novel isoforms of human spermatogenesis associated gene SPATA3. Mol Biol Rep 46: 3827-3834, 2019.
29. Girault MS, Dupuis S, Ialy-Radio C, Stouvenel L, Viollet C, Pierre R, Favier M, Ziyyat A and Barbaux S: Deletion of the Spata3 gene induces sperm alterations and in vitro hypofertility in mice. Int J Mol Sci 22: 1959, 2021.
30. Li M, Ma Q, Gong T, Zhang Y, Yan P, Zhai X and Guo R: Bioinformatics analysis and primary identification of the structure and function of mouse Spata3 protein. Acta Laboratorium Animalis Scientia Sinica 30: 767-776, 2022 (In Chinese).
31. Li L, Liu G, Fu JJ, Li LY, Tan XJ, Yang S and Lu GX: Molecular cloning and characterization of a novel transcript variant of Mtsarg1 gene. Mol Biol Rep 36: 1023-1032, 2009.
32. Wang Y, Wen L, Bai X, Cao R, Wang H and Guo R: Novel expression of spermatogenesis-associated protein 3 gene in mouse spermatogenic cells and its influence upon apoptosis and autophagy in HEK 293T cells. Acta Anatomica Sinica 1: 41-48, 2018 (In Chinese).
33. Choi S, Cho N and Kim KK: The implications of alternative pre-mRNA splicing in cell signal transduction. Exp Mol Med 55: 755-766, 2023.
34. Carey KT and Wickramasinghe VO: Regulatory potential of the RNA processing machinery: Implications for human disease. Trends Genet 34: 279-290, 2018.
35. Venables JP: Alternative splicing in the testes. Curr Opin Genet Dev 12: 615-619, 2002.
36. Zhao F, Yan Y, Wang Y, Liu Y and Yang R: Splicing complexity as a pivotal feature of alternative exons in mammalian species. BMC Genomics 24: 198, 2023.
37. Yang X, Coulombe-Huntington J, Kang S, Sheynkman GM, Hao T, Richardson A, Sun S, Yang F, Shen YA, Murray RR, *et al*: Widespread expansion of protein interaction capabilities by alternative splicing. Cell 164: 805-817, 2016.
38. Romeo-Cardeillac C, Trovero MF, Radío S, Smircich P, Rodríguez-Casuriaga R, Geisinger A and Sotelo-Silveira J: Uncovering a multitude of stage-specific splice variants and putative protein isoforms generated along mouse spermatogenesis. BMC Genomics 25: 295, 2024.
39. Baralle FE and Giudice J: Alternative splicing as a regulator of development and tissue identity. Nat Rev Mol Cell Biol 18: 437-451, 2017.
40. Naro C, Cesari E and Sette C: Splicing regulation in brain and testis: Common themes for highly specialized organs. Cell Cycle 20: 480-489, 2021.
41. Li Q, Li T, Xiao X, Ahmad DW, Zhang N, Li H, Chen Z, Hou J and Liao M: Specific expression and alternative splicing of mouse genes during spermatogenesis. Mol Omics 16: 258-267, 2020.
42. Legrand JMD and Hobbs RM: RNA processing in the male germline: Mechanisms and implications for fertility. Semin Cell Dev Biol 79: 80-91, 2018.
43. Fu J, Cheng J, Zhou Q, Khan MA, Duan C, Peng J, Lv H and Fu J: Novel compound heterozygous nonsense variants, p.L150* and p.Y3565*, of the USH2A gene in a Chinese pedigree are associated with Usher syndrome type IIA. Mol Med Rep 22: 3464-3472, 2020.
44. Alzahayqa M, Jamous A, Khatib AAH and Salah Z: TET1 isoforms have distinct expression pattern, localization and regulation in breast cancer. Front Oncol 12: 848544, 2022.
45. Pereira CD, Serrano JB, Martins F, da Cruz E Silva OAB and Rebelo S: Nuclear envelope dynamics during mammalian spermatogenesis: New insights on male fertility. Biol Rev Camb Philos Soc 94: 1195-1219, 2019.
46. Ohkura H: Meiosis: An overview of key differences from mitosis. Cold Spring Harb Perspect Biol 7: a015859, 2015.
47. Waclawska A and Kurpisz M: Key functional genes of spermatogenesis identified by microarray analysis. Syst Biol Reprod Med 58: 229-235, 2012.
48. Ramm SA, Schärer L, Ehmcke J and Wistuba J: Sperm competition and the evolution of spermatogenesis. Mol Hum Reprod 20: 1169-1179, 2014.
49. Guo X: Localized proteasomal degradation: From the nucleus to cell periphery. Biomolecules 12: 229, 2022.
50. Brooks P, Fuertes G, Murray RZ, Bose S, Knecht E, Rechsteiner MC, Hendil KB, Tanaka K, Dyson J and Rivett J: Subcellular localization of proteasomes and their regulatory complexes in mammalian cells. Biochem J 346 (Pt 1): 155-161, 2000.
51. Morgan M, Kumar L, Li Y and Baptissart M: Post-transcriptional regulation in spermatogenesis: All RNA pathways lead to healthy sperm. Cell Mol Life Sci 78: 8049-8071, 2021.
52. Bettegowda A and Wilkinson MF: Transcription and post-transcriptional regulation of spermatogenesis. Philos Trans R Soc Lond B Biol Sci 365: 1637-1651, 2010.
53. Boulikas T: Putative nuclear localization signals (NLS) in protein transcription factors. J Cell Biochem 55: 32-58, 1994.
54. Jiang X, Wu M, Albo J and Rao Q: Non-specific binding and cross-reaction of ELISA: A case study of porcine hemoglobin detection. Foods 10: 1708, 2021.
55. Lander ES, Linton LM, Birren B, Nusbaum C, Zody MC, Baldwin J, Devon K, Dewar K, Doyle M, FitzHugh W, *et al*: Initial sequencing and analysis of the human genome. Nature 409: 860-921, 2001.
56. Moritz L and Hammoud SS: The art of packaging the sperm genome: Molecular and structural basis of the histone-to-protamine exchange. Front Endocrinol (Lausanne) 13: 895502, 2022.
57. Zhou J, Du YR, Qin WH, Hu YG, Huang YN, Bao L, Han D, Mansouri A and Xu GL: RIM-BP3 is a manchette-associated protein essential for spermiogenesis. Development 136: 373-382, 2009.
58. Piechka A, Sparanese S, Witherspoon L, Hach F and Flannigan R: Molecular mechanisms of cellular dysfunction in testes from men with non-obstructive azoospermia. Nat Rev Urol 21: 67-90, 2024.

59. Martianov I, Fimia GM, Dierich A, Parvinen M, Sassone-Corsi P and Davidson I: Late arrest of spermiogenesis and germ cell apoptosis in mice lacking the TBP-like TLF/TRF2 gene. Mol Cell 7: 509-515, 2001.
60. Xu L, Lu Y, Han D, Yao R, Wang H, Zhong S, Luo Y, Han R, Li K, Fu J, *et al*: Rnf138 deficiency promotes apoptosis of spermatogonia in juvenile male mice. Cell Death Dis 8: e2795, 2017.
61. Siebert-Kuss LM, Krenz H, Tekath T, Wöste M, Di Persio S, Terwort N, Wyrwoll MJ, Cremers JF, Wistuba J, Dugas M, *et al*: Transcriptome analyses in infertile men reveal germ cell-specific expression and splicing patterns. Life Sci Alliance 6: e202201633, 2022.
62. Giassetti MI, Miao D, Law NC, Oatley MJ, Park J, Robinson LD, Maddison LA, Bernhardt ML and Oatley JM: ARRDC5 expression is conserved in mammalian testes and required for normal sperm morphogenesis. Nat Commun 14: 2111, 2023.
63. Hermann BP, Cheng K, Singh A, Roa-De La Cruz L, Mutoji KN, Chen IC, Gildersleeve H, Lehle JD, Mayo M, Westernströer B, *et al*: The mammalian spermatogenesis single-cell transcriptome, from spermatogonial stem cells to spermatids. Cell Rep 25: 1650-1667.e1658, 2018.
64. Anbazhagan R, Kavarthapu R, Dale R, Campbell K, Faucz FR and Dufau ML: miRNA expression profiles of mouse round spermatids in GRTH/DDX25-mediated spermiogenesis: mRNA-miRNA network analysis. Cells 12: 756, 2023.